

EPR Spectroscopic Trapping of the Active Species of Nonheme Iron-Catalyzed Oxidation

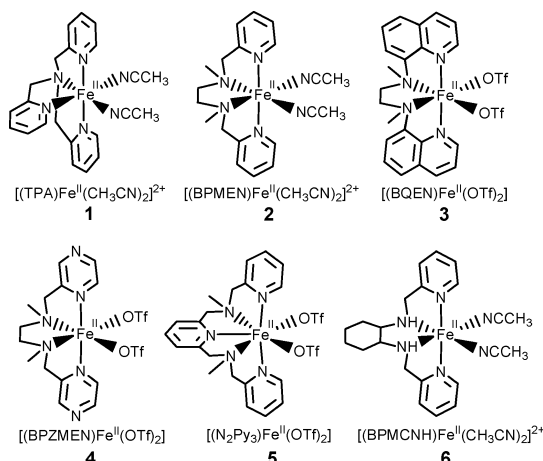
Oleg Y. Lyakin,[†] Konstantin P. Bryliakov,[†] George J. P. Britovsek,[‡] and Evgenii P. Talsi^{*†}

Siberian Branch of the Russian Academy of Sciences, Boreskov Institute of Catalysis, Novosibirsk 630090, Pr. Lavrentieva 5, Russia, and Department of Chemistry, Imperial College London, London SW7 2AY, Exhibition Road, U.K.

Received April 3, 2009; E-mail: talsi@catalysis.ru

Recently, substantial research efforts have been aimed at the development of catalyst systems capable to induce oxygen-transfer reactions similar to those of typical monooxygenase enzymes, including alkene epoxidation and alkane hydroxylation.^{1,2} The most efficient iron-based bioinspired olefin epoxidation catalysts presently known, which use H₂O₂(CH₃CO₃H) as oxidant, are iron complexes with aminopyridine ligands, [(TPA)Fe^{II}(CH₃CN)₂](ClO₄)₂ (**1**) and [(BPMEN)Fe^{II}(CH₃CN)₂](ClO₄)₂ (**2**) (Chart 1).³ Despite intensive research efforts, the nature of the critical oxidant(s) in catalytic systems such as **1**/H₂O₂(CH₃CO₃H) and **2**/H₂O₂(CH₃CO₃H) remains elusive.⁴ Oxoiron(IV) complexes of the type [(L)Fe^{IV}=O(S)]²⁺, which are reactive toward alkenes, were observed in the catalytic systems **1,2**/CH₃CO₃H (L = TPA or BPMEN, S = H₂O or CH₃CN).⁵ However, the independently determined selectivity of [(TPA)Fe^{IV}=O(S)]²⁺ toward epoxidation of olefins is poor and cannot explain the observed yield of epoxide in the catalyst system **1**/CH₃CO₃H/cyclooctene.³ Therefore, another more selective species should drive epoxidation. Here, we report on the EPR detection of these very unstable and highly reactive iron–oxygen intermediates in the catalyst systems **1,2**/*m*-CPBA, **1,2**/CH₃CO₃H, and **2**/H₂O₂, (*m*-CPBA = *meta*-chloroperoxybenzoic acid). Several related systems, **3–6**/*m*-CPBA and **3–6**/CH₃CO₃H, have been included in the present study (Chart 1).

Chart 1



The EPR spectrum of a sample frozen to $-196\text{ }^{\circ}\text{C}$ after mixing **1** with *m*-CPBA at $-60\text{ }^{\circ}\text{C}$ for 30 s and storing at $-70\text{ }^{\circ}\text{C}$ ($[\mathbf{1}] = 0.04\text{ M}$, $[m\text{-CPBA}]/[\mathbf{1}] = 2$) shows signals of a new complex **1a** with *g*-values of $g_1 = 2.71$, $g_2 = 2.42$, $g_3 = 1.53$. The maximum concentration of **1a** amounts to 15% of total iron concentration.

Self-decay of **1a** follows first-order kinetics with an apparent rate constant of $(1.6 \pm 0.2) \times 10^{-3}\text{ s}^{-1}$ at $-70\text{ }^{\circ}\text{C}$ (Figure 1). The rate of this decay increases by a factor of 5 in the presence of 12 equiv of cyclohexene, thus indicating that **1a** is reactive toward cyclohexene even at $-70\text{ }^{\circ}\text{C}$ (Figure S1, Supporting Information (SI)). The only reaction product formed after storing the sample above at $-70\text{ }^{\circ}\text{C}$ for 1 h is cyclohexene oxide (yield 80% with respect to **1**; see SI for experimental details). Decay of **1a** is accelerated with increasing cyclohexene concentration. Addition of electron-deficient olefins to the **1**/*m*-CPBA system does not substantially affect the decay rate of **1a** (Table S1). The same complex **1a** was observed by EPR in the system **1**/CH₃CO₃H. The maximum concentration of **1a** amounts to 7% of $[\text{Fe}]_{\text{total}}$ (Table S2).

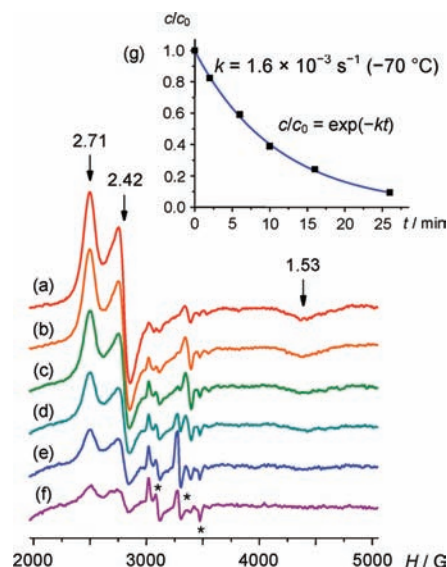


Figure 1. X-band EPR spectra ($-196\text{ }^{\circ}\text{C}$) of the sample **1**/*m*-CPBA frozen after mixing the reagents during 30 s at $-60\text{ }^{\circ}\text{C}$ in a 1.7:1 CH₂Cl₂/CH₃CN mixture ($[\mathbf{1}] = 0.04\text{ M}$, $[m\text{-CPBA}] = 0.08\text{ M}$) and storing at $-70\text{ }^{\circ}\text{C}$ for (a) 0, (b) 2, (c) 6, (d) 10, (e) 16, and (f) 26 min. Signals denoted by asterisks belong to still unidentified minor species. (g) Relative concentration of **1a** (c/c_0) vs time calculated from the decay of EPR signals of **1a** in (a)–(f).

The catalytic systems **1**/CH₃CO₃H and **2**/CH₃CO₃H display similar reactivity patterns toward epoxidation of cyclooctene.³ EPR studies on the systems **2**/CH₃CO₃H and **2**/*m*-CPBA give results similar to those for systems based on complex **1**. EPR spectra of **2**/CH₃CO₃H and **2**/*m*-CPBA systems, frozen to $-196\text{ }^{\circ}\text{C}$ at various moments of time after mixing the reagents at $-60\text{ }^{\circ}\text{C}$ and storing at $-70\text{ }^{\circ}\text{C}$, shows that complex **2a** displays a rhombic EPR spectrum ($g_1 = 2.69$, $g_2 = 2.42$, $g_3 = 1.70$) (Figure S2). The intensities of these three peaks change in parallel. The apparent rate constant evaluated for the self-decay of **2a** at $-70\text{ }^{\circ}\text{C}$ is (5.4

[†] Boreskov Institute of Catalysis.

[‡] Imperial College London.

$\pm 1.3) \times 10^{-4} \text{ s}^{-1}$. The rate of this decay increases by a factor of 10 in the presence of 12 equiv of cyclohexene. Thus, both **1a** and **2a** are reactive toward cyclohexene even at -70°C .

To establish that intermediate **2a** does indeed drive the catalytic cyclohexene epoxidation by catalyst system **2**/ H_2O_2 , we have compared the yield of cyclohexene oxide formed in the catalyst system **2**/ H_2O_2 /cyclohexene at -70°C ($[\mathbf{2}] = 0.027 \text{ M}$, $[\text{H}_2\text{O}_2] = 0.27 \text{ M}$, $[\text{cyclohexene}] = 0.81 \text{ M}$) with that expected from the kinetic data for **2a**. The EPR spectra of the above catalyst system in the absence of cyclohexene show that the concentration of **2a** is practically constant during 1 h at -70°C and amounts to $(2.0 \pm 0.8) \times 10^{-3} \text{ M}$ (Figure S3). In order for the concentration of **2a** to reach a steady state, its rate of formation, $W_{\text{F}(\mathbf{2a})}$, must equal its rate of decay, $W_{\text{F}(\mathbf{2a})} = k \times [\mathbf{2a}]$, where k is the rate constant of self-decay of **2a** at -70°C , and $[\mathbf{2a}]$ is the steady state concentration of **2a** in the absence of cyclohexene. In the presence of cyclohexene, **2a** cannot be detected, in agreement with its high reactivity toward cyclohexene at -70°C (Figure S4). Hence, the rate of formation of cyclohexene oxide is expected to be equal to the rate of **2a** formation ($W_{\text{F}(\text{epoxide})} = W_{\text{F}(\mathbf{2a})}$). The expected concentration of cyclohexene oxide formed during t seconds of the catalytic reaction is given by following equation

$$[\text{cyclohexene oxide}] = k \times [\mathbf{2a}] \times t \quad (1)$$

Values of $k = (5.4 \pm 1.3) \times 10^{-4} \text{ s}^{-1}$ and $[\mathbf{2a}] = (2.0 \pm 0.8) \times 10^{-3} \text{ M}$, derived from our measurements, would thus predict that the cyclohexene oxide formed during 1 h of the catalytic reaction at -70°C (eq 1) should reach a concentration of $(3.9 \pm 2.5) \times 10^{-3} \text{ M}$. Experimentally, a concentration of cyclohexene oxide of $7.4 \times 10^{-3} \text{ M}$ was determined by gas chromatographic product analysis (see SI for details). That the predicted and experimental epoxide yields are close strongly supports the key role of **2a** in selective epoxidation. The results of catalytic cyclohexene epoxidation by systems **1,2**/ $\text{CH}_3\text{CO}_3\text{H}(m\text{-CPBA})$ are presented in Table S3.

To view the role of intermediates such as **1a** and **2a** in a broader perspective, we have compared the reactivity patterns of complexes **1–6** with regard to cyclohexene epoxidation by H_2O_2 . The results of these studies (Table S4) show that only the systems **1–4**/ H_2O_2 demonstrate epoxidation activity at 25°C . Interestingly, intermediates of the type **1a**, **2a**, **3a**, and **4a**, with EPR parameters presented in Table S5, were observed only in systems **1–4**/ $\text{CH}_3\text{CO}_3\text{H}$ and **1–4**/ $m\text{-CPBA}$ (Figures 1, S2, and S5). In the systems **5,6**/ $m\text{-CPBA}$ and **5,6**/ $\text{CH}_3\text{CO}_3\text{H}$, the only unidentified signal near $g = 4$ is observed.

Intermediates **1a** and **2a** display EPR spectra characteristic of $S = 1/2$ species. Several iron–oxygen intermediates, most notably species of the type $\text{Fe}^{\text{III}}\text{—OOC(O)R}^6$ and $\text{Fe}^{\text{V}}\text{=O}^7$ can in principle exhibit such EPR spectra (Table S5) and should thus be considered as potential structural models. An assignment of **1a** and **2a** to low-spin acylperoxo complexes of the type $[(\text{L})\text{Fe}^{\text{III}}(\text{OOC(O)R})(\text{S})]^{2+}$ can be excluded, since the EPR parameters of complexes $[(\text{L})\text{Fe}^{\text{III}}(\text{OOR})(\text{S})]^{2+}$ are sensitive to the nature of R' (H or $t\text{Bu}$) (Table S5). However, one and the same complex **2a** was observed in the systems **2**/ $m\text{-CPBA}$, **2**/ $\text{CH}_3\text{CO}_3\text{H}$, and **2**/ H_2O_2 . The only reasonable possibility thus appears to be that **1a** and **2a** are low-spin oxoiron(V) intermediates of the type $[(\text{TPA})\text{Fe}^{\text{V}}\text{=O}(\text{S})]^{3+}$ and $[(\text{BPMEN})\text{Fe}^{\text{V}}\text{=O}(\text{S})]^{3+}$, respectively ($\text{S} = \text{H}_2\text{O}$ or CH_3CN).

Synthesis of the first and so far only bona fide example of an oxoiron(V) complex, $[(\text{TAML})\text{Fe}^{\text{V}}\text{=O}]^-$, where TAML is a macrocyclic tetraamide ligand, was reported in 2007. The EPR spectra observed for **1a** and **2a** differ distinctly from the EPR spectrum reported for $[(\text{TAML})\text{Fe}^{\text{V}}\text{=O}]^-$ ($g_1 = 1.99$, $g_2 = 1.97$, $g_3 = 1.74$).⁷ This difference can be caused by diverse ligand fields. The most specific spectral feature of $[(\text{TAML})\text{Fe}^{\text{V}}\text{=O}]^-$ (distinguishing it from Fe^{III} and $\text{Fe}^{\text{III}}\text{Fe}^{\text{IV}}$ species found in the systems based on **1** and **2**) is the high-field peak at $g = 1.74$. This peak is much broader than those at $g = 1.97$ and 1.99 .⁷ Similar peaks at $g = 1.70$ and 1.53 were observed for $[(\text{BPMEN})\text{Fe}^{\text{V}}\text{=O}(\text{S})]^{3+}$ and $[(\text{TPA})\text{Fe}^{\text{V}}\text{=O}(\text{S})]^{3+}$, respectively (Figures 1 and S2). These peaks are much broader than the corresponding low-field peaks, as in the case of $[(\text{TAML})\text{Fe}^{\text{V}}\text{=O}]^-$. However, it is evident that further studies are needed for the unambiguous assignment of the observed intermediates to the oxoiron(V) species.

The main value of this paper is EPR spectroscopic trapping of the actual epoxidizing agents of bioinspired catalyst systems based on nonheme iron complexes and hydrogen peroxide. Despite the nature of these iron–oxygen species is not entirely clear, their key role in epoxidation has been reliably established.

Acknowledgment. The authors thank the Russian Foundation for Basic Research, Grants 06-03-32214 and 09-03-00087, for financial support. We are grateful to Prof. Dr. Hans Brintzinger for fruitful comments.

Supporting Information Available: Detailed experimental procedures, EPR spectra, Table S1 of the influence of olefin addition on the decay of **1a**, Table S2 of maximum concentration of **1a** and **2a**, Tables S3 and S4 of epoxide yields for cyclohexene oxidations, Table S5 of EPR spectroscopic parameters for $S = 1/2$ iron–oxygen species. This material is available free of charge via the Internet at <http://pubs.acs.org>.

References

- (1) (a) Costas, M.; Mehn, M. P.; Jensen, M. P.; Que, L., Jr. *Chem. Rev.* **2004**, *104*, 939–986. (b) Tshuva, E. Y.; Lippard, S. J. *Chem. Rev.* **2004**, *104*, 987–1012. (c) Kryatov, S. V.; Rybak-Akimova, E. V.; Schindler, S. *Chem. Rev.* **2005**, *105*, 2175–2226. (d) Que, L., Jr.; Tolman, W. B. *Nature* **2008**, *455*, 333–340.
- (2) (a) Chen, K.; Que, L., Jr. *J. Am. Chem. Soc.* **2001**, *123*, 6327–6337. (b) Chen, K.; Costas, M.; Kim, J.; Tipton, A. K.; Que, L., Jr. *J. Am. Chem. Soc.* **2002**, *124*, 3026–3035. (c) Costas, M.; Que, L., Jr. *Angew. Chem., Int. Ed.* **2002**, *41*, 2179–2181. (d) Bukowski, M. R.; Comba, P.; Lienke, A.; Limberg, C.; de Laorden, C. L.; Mas-Ballesté, R.; Merz, M.; Que, L., Jr. *Angew. Chem., Int. Ed.* **2006**, *45*, 3446–3449. (e) Taktak, S.; Kryatov, S. V.; Haas, T. E.; Rybak-Akimova, E. V. *J. Mol. Catal. A: Chem.* **2006**, *259*, 24–34. (f) Company, A.; Gómez, L.; Güell, M.; Ribas, X.; Luis, J. M.; Que, L., Jr.; Costas, M. *J. Am. Chem. Soc.* **2007**, *129*, 15766–15767.
- (3) Mas-Ballesté, R.; Que, L., Jr. *J. Am. Chem. Soc.* **2007**, *129*, 15964–15972.
- (4) (a) Chen, K.; Que, L., Jr. *Chem. Commun.* **1999**, 1375–1376. (b) Kaizer, J.; Klinker, E. J.; Oh, N. Y.; Rohde, J.-U.; Song, W. J.; Stubna, A.; Kim, J.; Münck, E.; Nam, W.; Que, L., Jr. *J. Am. Chem. Soc.* **2004**, *126*, 472–473. (c) Jensen, M. P.; Costas, M.; Ho, Y. N.; Kaizer, J.; Mairata i Payeras, A.; Münck, E.; Que, L., Jr.; Rohde, J.-U.; Stubna, A. *J. Am. Chem. Soc.* **2005**, *127*, 10512–10525. (d) Oh, N. Y.; Seo, M. S.; Lim, M. H.; Consugar, M. B.; Park, M. J.; Rohde, J.-U.; Han, J.; Kim, K. M.; Kim, J.; Que, L., Jr. *Chem. Commun.* **2005**, 5644–5646. (e) Thibon, A.; England, J.; Martinho, M.; Young, V. G., Jr.; Frisch, J. R.; Guillot, R.; Gierd, J.-J.; Münck, E.; Que, L., Jr.; Banse, F. *Angew. Chem., Int. Ed.* **2008**, *47*, 7064–7067.
- (5) (a) Lim, M. H.; Rohde, J.-U.; Stubna, A.; Bukowski, M. R.; Costas, M.; Ho, R. Y. N.; Münck, E.; Nam, W.; Que, L., Jr. *Proc. Natl. Acad. Sci. U.S.A.* **2003**, *100*, 3665–3670. (b) Duban, E. A.; Bryliakov, K. P.; Talsi, E. P. *Eur. J. Inorg. Chem.* **2007**, 852–857.
- (6) Yamaguchi, K.; Watanabe, Y.; Morishima, I. *J. Am. Chem. Soc.* **1993**, *115*, 4058–4065.
- (7) de Oliveira, F. T.; Chanda, A.; Banerjee, D.; Shan, X.; Mondal, S.; Que, L., Jr.; Bominaar, E. L.; Münck, E.; Collins, T. J. *Science* **2007**, *315*, 835–838.

JA902659C